Gas Separation Hot Paper

International Edition: DOI: 10.1002/anie.201905014
German Edition: DOI: 10.1002/ange.201905014

Decorated Traditional Zeolites with Subunits of Metal–Organic Frameworks for CH_4/N_2 Separation

Yaqi Wu, Danhua Yuan, Dawei He, Jiacheng Xing, Shu Zeng, Shutao Xu, Yunpeng Xu, and Zhongmin Liu**

Dedicated to the 70th anniversary of the Dalian Institute of Chemical Physics, CAS

Abstract: *Metal–organic frameworks (MOF) materials are promising materials for gas separation, but their application still faces various challenges. A strategy is now reported for introducing subunits of MOFs into traditional zeolite frameworks to obtain applicable adsorbents with advantages of both zeolites and MOFs. The subunits of ZIFs were introduced into zeolite Y and zeolite ZSM-5 for CH_4/N_2 separation. Both the molecular simulation and experimental results validated that the IAST CH_4/N_2 selectivity of the resulting samples greatly improved (above 8, at 100 kPa and 25 °C) with the incorporation of ZIF subunits into zeolites structure, and the selectivities were obviously higher than that of zeolites and even better than that of ZIFs. This strategy not only gave rise to an efficient adsorbent for CH_4/N_2 separation but also provided ideas for design of other adsorption and separation materials.*

Metal–organic frameworks (MOFs) have rapidly emerged as advanced crystalline porous materials in the last two decades. Owing to their ultrahigh surface areas, tunable porosities, and adjustable surface group functionalities, MOFs exhibit high adsorption capacity towards various gases as well as high selectivity towards many gas mixtures.[1] Therefore, MOFs show great potential as selective adsorbents, particularly in some difficult separation systems, such as CH_4/N_2, $C_2H_2/C_2H_4/C_2H_6$, and isomers of xylene.[2] Among these systems, CH_4/N_2 separation is one of the most challenging endeavors in gas separation which is of particular importance in natural gas utilization.[3] The development of efficient selective adsorbents can solve the highly energy-consuming problems caused by the current method of cryogenic distillation. However, most of the traditional porous materials including zeolites do not show sufficient separation towards CH_4/N_2 for industrial application because of the very similar properties of methane and nitrogen molecules in terms of diameter, polarity, and so on. Furthermore, previous studies have shown that zeolitic imidazolate frameworks (ZIFs), a particularly interesting class of MOFs, exhibited preferential CH_4 adsorption over N_2.[4] Theoretical studies revealed that the preferential adsorption sites for CH_4 on ZIF-8 are located in specific regions close to the organic imidazolate linker, suggesting that the imidazolate linkers facilitate the adsorption of methane.[5] Inspired by the reported theoretical results, herein, we report a strategy by introducing ZIF-8 subunits, ZIF-14 subunits, and their derivatives into traditional zeolites to increase the CH_4/N_2 selectivity of traditional zeolites. The low cost and mature synthesis technology of zeolites make it possible for this strategy to overcome the problems faced by MOFs, such as complicated synthesis processes, high costs, and forming difficulties, and to realize the combination of advanced MOFs and traditional zeolites. ZIF-8 subunits (Zn-mIM, mIM = 2-methylimidazole), ZIF-14 subunits (Zn-eIM, eIM = 2-ethylimidazole), and their derivatives Zn-pIM (pIM = 2-propylimidazole) were used to decorate zeolite Y and zeolite ZSM-5.

The interaction energies (IE) between the adsorbent and adsorbate molecules were obtained by density functional theory (DFT) calculations (see the Supporting Information). The Si1Al1 cluster was adopted as the zeolite framework model.[6] The optimized conformational geometries and interaction energies between adsorbate molecule of methane or nitrogen and adsorbent clusters of Zn^{2+}/Si1Al1, Zn-mIM/Si1Al1, Zn-eIM/Si1Al1, and Zn-pIM/Si1Al1 are illustrated in Figure 1. It was indicated that the IE between CH_4 and decorated zeolite clusters (Zn-mIM/Si1Al1, Zn-eIM/Si1Al1, and Zn-pIM/Si1Al1) were much lower than those of the Zn^{2+}/Si1Al1 cluster, while the IE between N_2 and decorated zeolite clusters increased obviously, theoretically suggesting that with the decoration of the ZIF subunit, the Si1Al1 cluster has stronger electrostatic interactions with CH_4 and weaker electrostatic interactions with N_2. In other words, the incorporation of Zn-mIM, Zn-eIM, and Zn-pIM may result in higher CH_4/N_2 selectivity of zeolite.

First, the pristine zeolites (NaY or HZSM-5) were ion-exchanged to zinc form. Second, the as-prepared zinc form zeolites were reacted with the imidazoles (see the Supporting Information). A typical adsorbent prepared with NaY, ion-exchanged to ZnY form and then reacted with 2-methylimidazole, was denoted as ZnY-mIM (for 2-ethylimidazole and 2-

[*] Y. Wu, Dr. D. Yuan, D. He, J. Xing, S. Zeng, Prof. Dr. S. Xu, Prof. Dr. Y. Xu, Prof. Dr. Z. Liu
National Engineering Laboratory for Methanol to Olefins, Dalian National Laboratory for Clean Energy, Dalian Institute of Chemical Physics, Chinese Academy of Sciences
Dalian 116023 (P. R. China)
E-mail: xuyp@dicp.ac.cn
liuzm@dicp.ac.cn
Y. Wu, D. He, J. Xing, S. Zeng
University of Chinese Academy of Sciences
Beijing 100049 (China)
Supporting information and the ORCID identification number(s) for the author(s) of this article can be found under: https://doi.org/10.1002/anie.201905014.

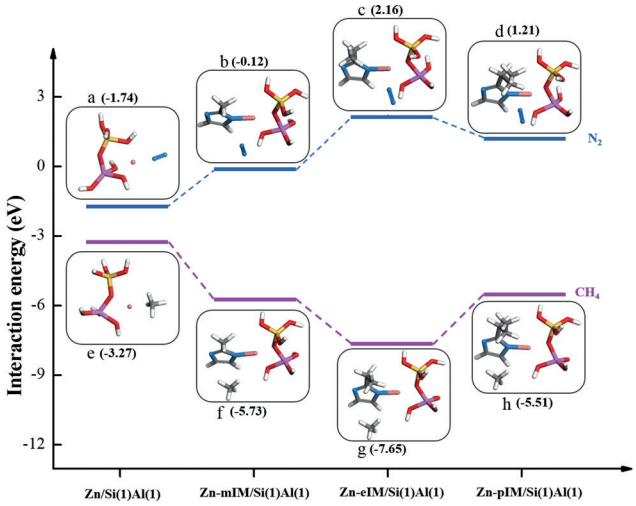

Figure 1. Optimized conformational geometries and simplified calculated interaction energies of a) N_2-Zn/Si(1)Al(1), b) N_2-Zn-mIM/Si-(1)Al(1), c) N_2-Zn-eIM/Si(1)Al(1), d) N_2-Zn-pIM/Si(1)Al(1), e) CH_4-Zn/Si(1)Al(1), (f) CH_4-Zn-mIM/Si(1)Al(1), g) CH_4-Zn-eIM/Si(1)Al(1), and h) CH_4-Zn-pIM/Si(1)Al(1). H white, O red, Si yellow, Al lavender, Zn pink, N blue, C gray.

propylimidazole, it would be ZnY-eIM and ZnY-pIM respectively). The proposed process and typical structures of the adsorbents are illustrated in Figure 2. For the first step, ^{23}Na MAS NMR spectra indicated that Zn^{2+} were exchanged with Na^+ inside the zeolite framework, confirming the existence of Zn^{2+} inside the zeolite framework (Supporting Information, Figure S2).[7] The Zn 2p XPS spectra (Supporting Information, Figure S3) exhibited the two characteristic peaks of Zn corresponding to Zn $2p_{1/2}$ and Zn $2p_{3/2}$, respectively, were observed for the resulting materials.[8] ^{23}Na MAS NMR, Zn 2p XPS, and ICP-OES (Supporting Information, Table S1) results confirmed the existence of Zn^{2+} inside the zeolite framework and the successful preparation of the zinc form zeolites. For the second step, it is the covalent binding of imidazoles and Zn^{2+} inside zeolite pores. In the FTIR spectra (Supporting Information, Figure S4), adsorption bands at 3138 cm^{-1}, 2979 cm^{-1}, 2935 cm^{-1}, 1473 cm^{-1}, and 1432 cm^{-1} could be attributed to C–H stretching and deformation

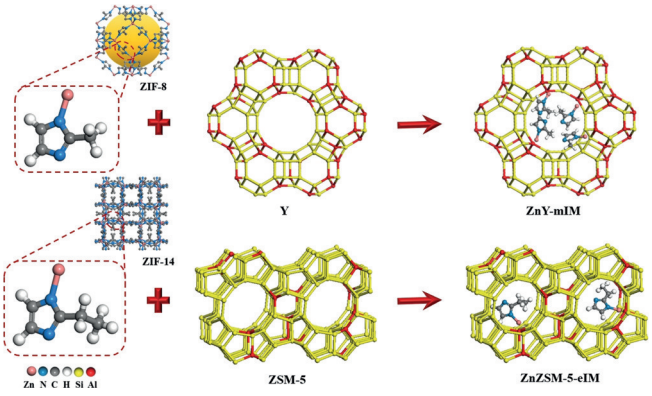

Figure 2. Illustration of zeolites decorated with ZIF-8 and ZIF-14 subunits.

vibrations of imidazole.[9] Additional bands at 1569 cm^{-1} can be assigned to C=N stretching vibration.[10] It can be seen that the imidazole characteristic IR bands of ZnY-mIM, ZnY-eIM, and ZnY-pIM matches well with that of ZIF-8. The absorption band at 420 cm^{-1} was observed for the Zn–N stretching vibration,[10a,11] indicating the covalent of imidazole and Zn^{2+} in the zeolite. The FTIR spectra results confirms that the functionalization of ZIF subunits into zeolite. ^{13}C CP/MAS NMR results of decorated samples also shown resonances which are the typical resonances of mIM, eIM, and pIM, respectively (Supporting Information, Figure S5).[12] The assignment of ^{15}N CP/MAS NMR signals has been made for pure imidazoles (mIM, eIM, and pIM) and ZIF-8 in Figure 3 and the Supporting Information, Figure S6.[13] For pure

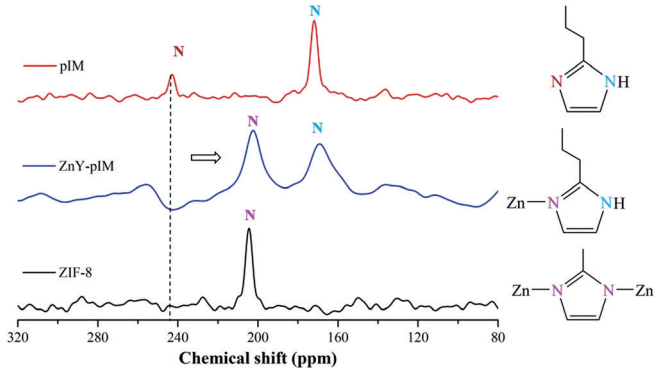

Figure 3. ^{15}N CP/MAS NMR spectra and assignment of N environment of pure pIM, ZnY-pIM, and ZIF-8.

imidazoles, two different N signals were observed. While for ZIF-8, both of the N in imidazole were linked with Zn, only a single resonance at 204.5 ppm appeared. Compared with pure imidazoles and ZIF-8, it was very clear that among the decorated adsorbents, two signals appeared, for which one of the resonance agreed well with the N of imidazoles in lower chemical shift, while the other was in accordance with the N of ZIF-8. Thus, for the decorated adsorbents, one of the N of imidazole bonded to Zn^{2+} and the other N remained the same chemical environment as pure imidazoles, implying the formation of ZIF subunits of Zn-IM. ^{13}C CP/MAS NMR spectra and ^{15}N CP/MAS NMR spectra further confirmed that zinc cations were existed inside the zeolite framework and the formation of ZIF subunit inside zeolite pores. Zn 2p XPS spectra demonstrated that the binding energy of decorated samples shifted toward lower values compared to pristine ZnY and close to ZIF-8, implying the formation of the ZIF fragment (Supporting Information, Figure S3). In HP-^{129}Xe NMR spectra (Supporting Information, Figure S7), the higher chemical shift of xenon were observed in ZnY-pIM and ZnZSM-5-pIM compared with ZnY and ZnZSM-5 indicated that xenon is adsorbed in a highly confined space, in other words, the pore size of the zeolites become smaller after the decoration.[14] Therefore, the entirety of the zeolite crystals are functionalized and not just the pore mouth. TEM images also indirectly suggested that the pore mouth also be functionalized (Supporting Information, Figure S8). The TGA results indicated that the combination of ZIF subunits

and zeolites were highly thermally stable (Supporting Information, Figure S9). The successful functionalization of ZIF subunit into zeolites can also be confirmed by elemental analysis and BET results (Supporting Information, Table S1). PXRD patterns indicated that major diffraction peaks of the decorated zeolites agreed well with the pristine zeolites, confirming that these zeolites remained intact after modification of the ZIF subunit (Supporting Information, Figures S10, S11). SEM images revealed no significant morphological changes in the zeolites after modification (Supporting Information, Figures S12, S13).

Figure 4 shows the CH_4 and N_2 adsorption isotherms of ZnY, ZnY-mIM, ZnY-eIM, ZnY-pIM, ZnZSM-5, ZnZSM-5-mIM, ZnZSM-5-eIM, and ZnZSM-5-pIM. CH_4/N_2 adsorption selectivities for equimolar CH_4/N_2 mixtures at 100 kPa and 25 °C of samples were calculated by ideal adsorbed solution theory (IAST) after isotherms were fit to the dual-site Langmuir–Freundlich equation (Supporting Information).[15] Fitting parameters and correlation coefficients of the DSLF isotherms are presented in the Supporting Information, Table S2. Compared with NaY (Supporting Information, Figure S14), CH_4 and N_2 uptake of ZnY (Figure 4 a,b) both decreased and CH_4/N_2 selectivity was almost unchanged. When modified with the mIM linker, the decrease in N_2 uptake was more than that in CH_4 uptake; thus, the CH_4/N_2 selectivity increased from 1.6 of pristine NaY and 2.1 of ZnY increased to 4.25. After modification of the eIM linker, the CH_4 uptake of the adsorbent (0.32 mmol g^{-1}, 100 kPa, 25 °C) was much higher than that of pristine ZnY (0.25 mmol g^{-1}, 100 kPa, 25 °C) while N_2 uptake decreased, which agreed well with the molecular simulation predictions. A higher CH_4/N_2 selectivity of 4.6 was achieved. When modified with the pIM linker, the bigger propyl group resulted in obvious decrease in CH_4 and N_2 uptakes. The decrease in N_2 uptake was more than that in CH_4 uptake and a high CH_4/N_2 selectivity of 7.56 was achieved. Furthermore, the CH_4/N_2 selectivity was higher than that of ZIF-8 (4.23) at 100 kPa and 25 °C (Supporting Information, Figure S15). It is reported that ZIF-14 cannot serve as a potential gas-sorption material owing to its small aperture (2.2 Å) and S_{BET} (28.7 $m^2 g^{-1}$).[16] Thus, ZIF-14 was not used as a reference in this work, while its subunit was used to decorate zeolites. Such an interesting phenomenon suggests that the strategy of decorating zeolite with the ZIF subunits to improve CH_4/N_2 selectivity achieved desirable results. The zeolite ZSM-5, CH_4 and N_2 uptake of zinc form varied slightly from HZSM-5 (Supporting Information, Figure S16) as well as CH_4/N_2 selectivity. After modification of the mIM, eIM, and pIM linkers, the CH_4 and N_2 uptake decreased; nevertheless, the amount of N_2 adsorbed was reduced dramatically from 0.22 mmol g^{-1} of ZnZSM-5 to 0.09 mmol g^{-1} of ZnZSM-5-mIM, 0.07 mmol g^{-1} ZnZSM-5-eIM, and 0.05 mmol g^{-1} ZnZSM-5-pIM at 100 kPa and 25 °C. Therefore, the CH_4/N_2 selectivities obviously increased from 4.25 for ZnZSM-5 to 5.94 for ZnZSM-5-mIM, 6.23 for ZnZSM-5-eIM, and 8.44 for ZnZSM-5-pIM at 100 kPa and 25 °C. CH_4/N_2 selectivities of the resulted samples are also quite comparable to the current top performing and typical materials (Supporting Information, Table S4). HP-^{129}Xe NMR spectra (Supporting Information, Figure S7) showed that compared with spectra of pristine zinc-form zeolites, the broadening linewidth of the decorated zeolites demonstrated the decrease of the mobility of xenon, which means the diffusion of the xenon was affected.[17] Adsorption kinetic curves exhibited that the CH_4 and N_2 uptake of the samples were all fast and soon reach to equilibrium (Supporting Information, Figure S17). Diffusion time constants (D/r^2) of CH_4 and N_2 also indicated that the diffusion of CH_4 and N_2 were slightly affected after the decoration (Supporting Information, Table S5). The resulted samples have good reproducibility and thermal stability as well (Supporting Information, Figures S18–S25). All the results indicated that the incorporation of ZIF subunits into traditional zeolites can greatly improve the CH_4/N_2 selectivity as expected from the molecular simulation results.

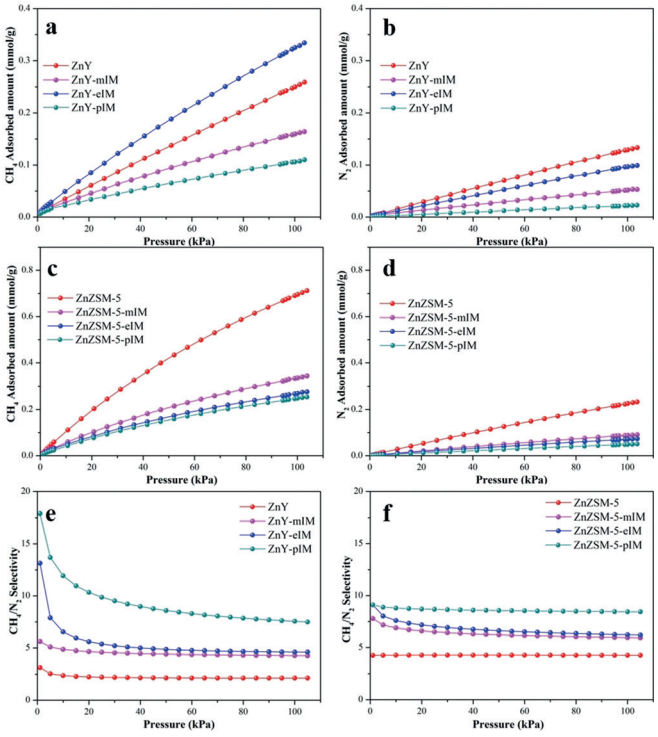

Figure 4. a),c) CH_4 and b),d) N_2 adsorption isotherms of samples at 25 °C. e),f) IAST-predicted selectivities for equimolar CH_4/N_2 mixtures on samples at 25 °C.

To evaluate the dynamic separation performances of the adsorbents, breakthrough experiments were carried out with CH_4/N_2/He (10:10:80) mixtures. Breakthrough curves of CH_4/N_2 mixtures on two typical samples of ZnY-pIM and ZnZSM-5-pIM are presented in Figure 5. For both of the adsorbents, N_2 firstly eluted from the packed bed whereas CH_4 was retained and then reached saturation. ZnY-pIM and ZnZSM-5-pIM exhibited efficient dynamic separation performances. Compared with pristine ZnY, the CH_4/N_2 dynamic separation performance was greatly enhanced (Supporting Information, Figure S26). The N_2 breakthrough of ZnY-eIM was slightly earlier than that of ZnY, while the breakthrough of CH_4 was much later. CH_4/N_2 separation performance of NaY was also poor than that of ZnY-eIM (Supporting Information, Figure S27). The cycle and regeneration capabilities of ZnY-pIM

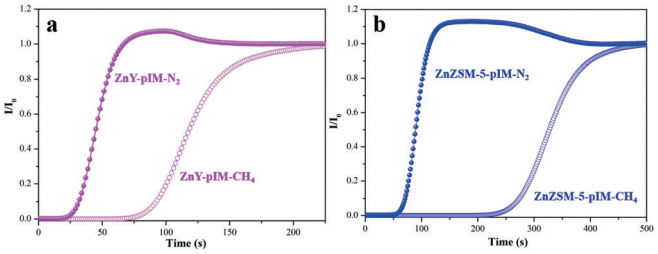

Figure 5. Breakthrough curves of CH_4/N_2/He (10/10/80) on ZnY-pIM and ZnZSM-5-pIM at 100 kPa and 25 °C.

and ZnZSM-5-pIM were further studied by breakthrough cycle experiments (Supporting Information, Figure S28).

In summary, we report a series of new adsorbents by introducing ZIF subunits into traditional zeolite Y and zeolite ZSM-5. Both the molecular simulation and experimental results indicate that the strategy of incorporating Zn-mIM, Zn-eIM, and Zn-pIM into zeolite Y and zeolite ZSM-5 resulted in significant enhancement in the CH_4/N_2 selectivity of the adsorbents, which were higher than those of pristine zeolites and even ZIFs. Notably, resulting adsorbents exhibited high thermal stability up to 500 °C and 600 °C, which makes the adsorbents very applicable. This strategy has combined traditional zeolites and MOFs perfectly, which can solve the complicated synthesis, high costs, and forming difficulties of MOFs as well as the problem of low CH_4/N_2 selectivity in traditional zeolites. This concept provides an idea for the design of new MOF–zeolite composite materials, ranging from various adsorbents to catalysts.

Acknowledgements

The work was supported by the National Key Research and Development Program of China (2016YFB0301603).

Conflict of interest

The authors declare no conflict of interest.

Keywords: gas adsorption · metal–organic frameworks · surface decoration · zeolites

How to cite: *Angew. Chem. Int. Ed.* **2019**, *58*, 10241 – 10244
Angew. Chem. **2019**, *131*, 10347 – 10350

[1] a) M. Eddaoudi, J. Kim, N. Rosi, D. Vodak, J. Wachter, M. O'Keeffe, O. M. Yaghi, *Science* **2002**, *295*, 469; b) R. Banerjee, A. Phan, B. Wang, C. Knobler, H. Furukawa, M. O'Keeffe, O. M. Yaghi, *Science* **2008**, *319*, 939.

[2] a) K. Lee, W. C. Isley, A. L. Dzubak, P. Verma, S. J. Stoneburner, L.-C. Lin, J. D. Howe, E. D. Bloch, D. A. Reed, M. R. Hudson, C. M. Brown, J. R. Long, J. B. Neaton, B. Smit, C. J. Cramer, D. G. Truhlar, L. Gagliardi, *J. Am. Chem. Soc.* **2014**, *136*, 698 – 704; b) L. Li, R.-B. Lin, R. Krishna, H. Li, S. Xiang, H. Wu, J. Li, W. Zhou, B. Chen, *Science* **2018**, *362*, 443; c) X. Cui, K. Chen, H. Xing, Q. Yang, R. Krishna, Z. Bao, H. Wu, W. Zhou, X. Dong, Y. Han, B. Li, Q. Ren, M. J. Zaworotko, B. Chen, *Science* **2016**, *353*, 141; d) V. Finsy, H. Verelst, L. Alaerts, D. De Vos, P. A. Jacobs, G. V. Baron, J. F. M. Denayer, *J. Am. Chem. Soc.* **2008**, *130*, 7110 – 7118.

[3] M. Tagliabue, D. Farrusseng, S. Valencia, S. Aguado, U. Ravon, C. Rizzo, A. Corma, C. Mirodatos, *Chem. Eng. J.* **2009**, *155*, 553 – 566.

[4] a) B. Liu, B. Smit, *J. Phys. Chem. C* **2010**, *114*, 8515 – 8522; b) H. Huang, W. Zhang, D. Liu, B. Liu, G. Chen, C. Zhong, *Chem. Eng. Sci.* **2011**, *66*, 6297 – 6305.

[5] a) H. Wu, W. Zhou, T. Yildirim, *J. Phys. Chem. C* **2009**, *113*, 3029 – 3035; b) J. Pérez-Pellitero, H. Amrouche, F. R. Siperstein, G. Pirngruber, C. Nieto-Draghi, G. Chaplais, A. Simon-Masseron, D. Bazer-Bachi, D. Peralta, N. Bats, *Chem. Eur. J.* **2010**, *16*, 1560 – 1571.

[6] a) Y. Kuwahara, K. Nishizawa, T. Nakajima, T. Kamegawa, K. Mori, H. Yamashita, *J. Am. Chem. Soc.* **2011**, *133*, 12462 – 12465; b) H. Yamashita, S. Takada, M. Hada, H. Nakatsuji, M. Anpo, *J. Photochem. Photobiol. A* **2003**, *160*, 37 – 42.

[7] M. Hunger, U. Schenk, A. Buchholz, *J. Phys. Chem. B* **2000**, *104*, 12230 – 12236.

[8] H. Chen, L. Wang, J. Yang, R. T. Yang, *J. Phys. Chem. C* **2013**, *117*, 7565 – 7576.

[9] a) R. Zhou, H. Wang, B. Wang, X. Chen, S. Li, M. Yu, *Ind. Eng. Chem. Res.* **2015**, *54*, 7516 – 7523; b) A. Bordoloi, S. Sahoo, F. Lefebvre, S. B. Halligudi, *J. Catal.* **2008**, *259*, 232 – 239.

[10] a) J. Liu, J. He, L. Wang, R. Li, P. Chen, X. Rao, L. Deng, L. Rong, J. Lei, *Sci. Rep.* **2016**, *6*, 23667; b) W. Xu, Z. Sun, H. Meng, Y. Han, J. Wu, J. Xu, Y. Xu, X. Zhang, *New J. Chem.* **2018**, *42*, 17429 – 17438.

[11] E. Shamsaei, Z.-X. Low, X. Lin, A. Mayahi, H. Liu, X. Zhang, J. Z. Liu, H. Wang, *Chem. Commun.* **2015**, *51*, 11474 – 11477.

[12] a) E. F. Baxter, T. D. Bennett, C. Mellot-Draznieks, C. Gervais, F. Blanc, A. K. Cheetham, *Phys. Chem. Chem. Phys.* **2015**, *17*, 25191 – 25196; b) J. Sánchez-Laínez, A. Veiga, B. Zornoza, S. R. G. Balestra, S. Hamad, A. R. Ruiz-Salvador, S. Calero, C. Téllez, J. Coronas, *J. Mater. Chem. A* **2017**, *5*, 25601 – 25608.

[13] a) K. Bouchmella, S. G. Dutremez, B. Alonso, F. Mauri, C. Gervais, *Cryst. Growth Des.* **2008**, *8*, 3941 – 3950; b) W. Morris, C. J. Stevens, R. E. Taylor, C. Dybowski, O. M. Yaghi, M. A. Garcia-Garibay, *J. Phys. Chem. C* **2012**, *116*, 13307 – 13312.

[14] a) Z. Qin, K. A. Cychosz, G. Melinte, H. El Siblani, J.-P. Gilson, M. Thommes, C. Fernandez, S. Mintova, O. Ersen, V. Valtchev, *J. Am. Chem. Soc.* **2017**, *139*, 17273 – 17276; b) S.-B. Liu, B. M. Fung, T.-C. Yang, E.-C. Hong, C.-T. Chang, P.-C. Shih, F.-H. Tong, T.-L. Chen, *J. Phys. Chem.* **1994**, *98*, 4393 – 4401.

[15] A. L. Myers, J. M. Prausnitz, *AIChE J.* **1965**, *11*, 121 – 127.

[16] X.-C. Huang, Y.-Y. Lin, J.-P. Zhang, X.-M. Chen, *Angew. Chem. Int. Ed.* **2006**, *45*, 1557 – 1559; *Angew. Chem.* **2006**, *118*, 1587 – 1589.

[17] a) F. Guenneau, K. Panesar, A. Nossov, M.-A. Springuel-Huet, T. Azaïs, F. Babonneau, C. Tourné-Péteilh, J.-M. Devoisselle, A. Gédéon, *Phys. Chem. Chem. Phys.* **2013**, *15*, 18805 – 18808; b) T. Azaïs, C. Tourné-Péteilh, F. Aussenac, N. Baccile, C. Coelho, J.-M. Devoisselle, F. Babonneau, *Chem. Mater.* **2006**, *18*, 6382 – 6390; c) S. Komulainen, J. Roukala, V. V. Zhivonitko, M. A. Javed, L. Chen, D. Holden, T. Hasell, A. Cooper, P. Lantto, V.-V. Telkki, *Chem. Sci.* **2017**, *8*, 5721 – 5727.

Manuscript received: April 22, 2019
Accepted manuscript online: May 20, 2019
Version of record online: June 17, 2019

